Thermomechanical analysis of a duplex plate subjected to a plasma major disruption

M.Akiyama
Department of Nuclear Engineering, University of Tokyo, Japan
K.Miya & H.Hashizume
Nuclear Engineering Research Laboratory, University of Tokyo, Japan
K.Ioki
Mitsubishi Atomic Power Industries, Japan

Abstract

To plasma interactive components of a fusion power reactor is deposited very high heat flux on a major plasma disruption categorized as abnormal operation, which would cause the consequent melting, evaporation and resolidification of the material. The event could result in metallurgical and mechanical deterioration of the material accompanied by high residual stress and small cracks. In the present study the thermomechanical behavior of a duplex plate which is one of most prospective candidates for the high heat flux component is analysed by a recently developed cmputer code based on FEM.

1. Introduction

Plasma interactive components of a fusion power reactor are subjected to heavy irradiation of high energy neutrons and high heat flux in normal operation. However, a large amount of heat is deposited to the components on a major plasma disruption categorized as abnormal operation. As a consequence of the event, the components melt to some extent of depth and then resolidify very quickly. The event could result in metallurgical and mechanical deterioration of material accompanied by high residual stress and small cracks.

This kind of thermomechanical behavior of the first wall was studied in [1,2,3]. Merrill et al. [1] discussed the melting based on a solution of heat conducting equation for the first wall with consideration of vaporization mass flux. Hassanein et al. [2] defined a sequence of the process as rapid heating, melting, intense evaporation, resolidification and cool-down, and calculated the detailed time history of the temperature distribution by solving a two moving boundary problem as well as the effect of vapor shielding on the melting. When the melting is caused by the disruption, the melt layer experiences electromagnetic force and may be affected by Rayleigh-Taylor instability. This was also discussed by Hassanein [3]. In [4] are solved surface melting and evaporation based on a comprehensive model including effects of vapor shielding, pulse shape and pulse duration. D. Sanzo developed an approximate analytical solution of the problem of melting and evaporation [5].

A duplex plate is a very prospective candidate for a high heat flux component such as a divertor plate. The plate is designed such that the front plate plays a role of protection of a rear plate against surface attack by charged particles with the high heat flux and the rear one does a role of heat sink.

Thermomechanical behavior of melting and resolidification of the duplex plate is thought very complicated because there is a case that melting point of an armor plate is much higher than that of the heat sink plate and the former is a catcher of the very high heat flux from a thermal quench of plasmas. Therefore there is such possibility that the heat sink material melts first and then the armor plate follows after it, and the latter resolidifies first. This phenomenon is dependent on design conditions such as heat removal by coolant, thicknesses of the plates, time constants of heat deposition, etc.

Such phenomena are analyzed numerically by the computer code based on FEM. The code has two parts where an equation of heat conduction is first solved and then elasto-plastic stress analysis is made to compute, for example, the residual stress. Numerical method is explained below, briefly.

2.Thermomechanical analysis of melting and resolidification

The present scheme starts to solve the following equation of heat conduction,

$$\rho\, c\, \dot{T} = k\, \nabla\, T + Q \qquad (1)$$

where ρ = density, c = specific heat per unit mass,
k = thermal conductivity, Q = heat generation rate, and
T = temperature, $\cdot = \partial/\partial t$, derivative in time

The conventional scheme of finite element formulation of eq. (1) is applied to derive the following system equation (see [6] for the detail),

$$[K]\{T\} + [C]\{\dot{T}\} = \{F\} \qquad (2)$$

where $\{F\}$ represents heat flux vector due to applied heat flux, bulk heat generation, radiation and heat tranfer. [C] and [K] represent specific heat matrix, and thermal conductivity matrix, respectively.

In order to apply eq. (2) to the melting phenomenon, some artificial technique is adopted. Although the temperature of the melting zone is kept constant T_m(= melting temperature), a very small increment of temperature, ΔT, is introduced in the zone. This means that the melted portion can be treated like a solid possesing a pseudo-specific heat capacity defined by $\Delta T/L$ (L is latent heat). If ΔT is very small, results could be expected accurate. In the following stress analysis, dependence of material properties on temperature is taken into account since the temperature exceeds the melting point. Also is used the Marcal iteration scheme in this analysis with the pseudo stress concept [8].

3. Numerical results

A model treated in this paper is a disk shape plate as shown in fig. 1 and consists of the coating material and stainless steel. Three kinds of materials are adopted to coat the base material of stainless steel. Radius and total thickness of the disk are 20 mm and 2.5 mm, respectively. The thickness of the coating material is kept constant h = 0.5 mm in the present analysis. A size of a heat spot is 10 mm in radius. Heat deposition during a plasma disruption is assumed to be step-wise with conditions of heat flux of q" = 200 MW/m^2 and duration time of 50 msec.

This situation simulates such a case that heat deposition from a thermal quench is localized very much to result in a very high heat flux of 200 MW/m^2. And no machanical boundary condition is applied except that displacement in r direction is zero at a central line of symmetry.

In fig. 2 are shown initiation and progress of the melting zone in a case of the coating material TiC and stainless steel. In this case, both TiC and SS316 start to melt almost at the same time. TiC has completed resolidification directly after termination of heat deposition while SS316 remains melted at the elapsed time of 75 msec.

In fig. 3 is shown melting behavior of SS316 coated with graphite. As well-known graphite does not melt but sublimates. In this case melting temperature of the graphite is presumed very high and only evaporation is taken into account. Radius of the melting zone is almost 10 mm. This is because the thickness of coating material is very thin.

In fig. 4 is shown melting behavior of Mo coated stainless steel. SS316 starts to melt at 25 msec when the coating material does not melt. SS316 does not melt at 25 msec in this cases of TiC and graphite coated stainless steel. This is due to high thermal conductivity of molybdenum compared with TiC and graphite. Molybdenum finishes resolidification right after the heat input termination.

In fig. 5 are shown temperature changes with time. The temperature of the coating material is taken at a surface of r = 0 and thus it is the highest. That of SS316 is taken at a contact surface with the coating material of r = 0. Temperature of the coating material starts to decrease rapidly right after the termination of heat input. That of SS316 starts to drop very gradually. In all cases, temperature of SS316 is higher than its melting point at the elapsed time of 80 msec and so melting layer still remains.

In fig. 6 is shown melting zone thickness of each material. The heat input amounts to 1000 Joule/cm^2 in all the cases ($200 \times 10^6 \times 50 \times 10^{-3} = 10 \times 10^6$ J $= 10$ MJ/m^2 $= \frac{10^7}{10^4} = 10^3$J/cm^2). Molybdenum melts much more deeper than TiC and maximum depths of both materials are 0.28 m and 0.175 mm, respectively. The depth is not large. Thus we may not need to worry about the melting if small cracks are not introduced. Although such a concern about the melting depends on the amount of heat input, cracking seems the most important problem as in terms of the consequence of a major plasma disruption if it deposites more heat than 1000 J/m^2. It is important to note that the melting depth of SS316 depends on a choice of the coating material and a combination with graphite gives the smallest one. A combination of TiC and Mo yields almost the same amount of melting depth.

In fig. 7 is shown evaporation thickness of the coating materials as a function of the elapsed time. Molybdenum shows the lowest value and graphite the largest one. In other words, loss of thickness due to plasma disruption can be negligible for Mo if the total frequency of the disruption can be assumed less than 1000 times, while it should be limited to less than 100 times for TiC and graphite.

In fig. 8 are shown stress distributions at various elapsed time. The stress is plotted on a A-B line shown in the figure and $\overline{AB}$ is just below the contact surface to locate in melted region in SS316. The stress in the range of r = 10 mm stays compressive until 20-30 msec. The stress in the melted region is zero which is seen from a curve of t = 50 msec. A curve of t = 3000 msec corresponds to a distribution of residual stress since the temperature distribution reduces to the initial one at the time. The maximum tensile stress is 220 MPa in this case. An important issue is whether or not this amount of residual stress is enough to cause cracking in SS316. This problem can be solved by doing experiment.

4.Conclusion

1) In designing the duplex plate we should be careful about strength of bonding between the plates after the plasma disruption so that we have to prepare data base on the strength from experiments.
2) The residual stress after melting followed by resolidification could be high to cause introduction of small cracks. This has been already verified by experiments for some structural material.

References

[1] B.J. Merrill & T.L. Jones; J. Nuc. Mater. 111 & 112 (1982)
[2] A.M. Hassanein, G.L. Kulcinski & W.C. Wolfer; J. Nuc. Mater. 111 & 112 (1982)
[3] W.G. Wolfer & A.M. Hassanein; J. Nuc. Mater. 111 & 112 (1982)
[4] A.M. Hassanein, G.L. Kulcinski & W.G. Wolfer; Nuc. Eng. Design/Fusion, 1 (1984)
[5] D. Sanzo; Nuc. Eng. Design/Fusion, 4 (1987)
[6] O.C. Zienkiewicz; Finite Element Method in Engineering Science (McGraw-Hill, N.Y. 1961)
[7] P.V. Marcal & I.P. King; Int. J. Mech. Sci. Vol.9 (1967)
[8] H. Hashizume, K. Miya & M. Seki; Nuc. Eng. Design/Fusion, to be published as a special issue.

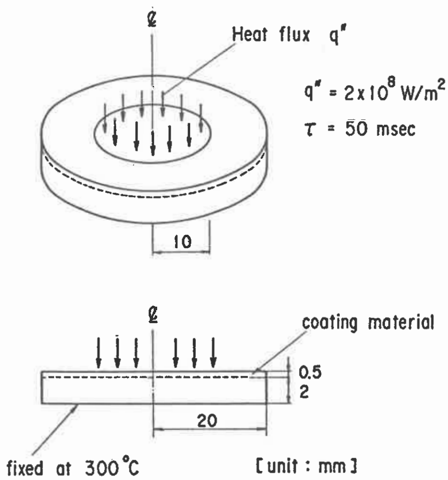

Fig. 1 Configuration of disk and heat input

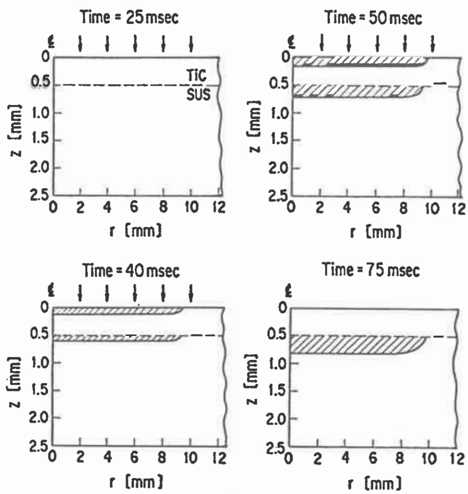

Fig. 2 Progress of melted zone (TiC-SUS)

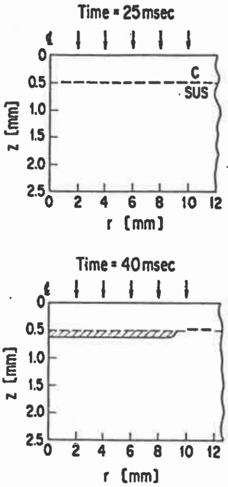

Fig. 3 Progress of melted zone
(Graphite-SUS)

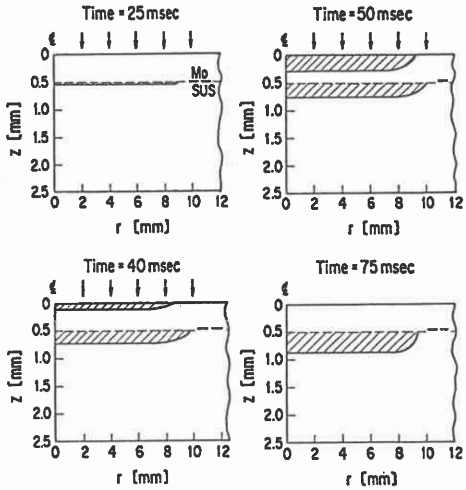

Fig. 4 Progress of melted zone
(Mo-SUS)

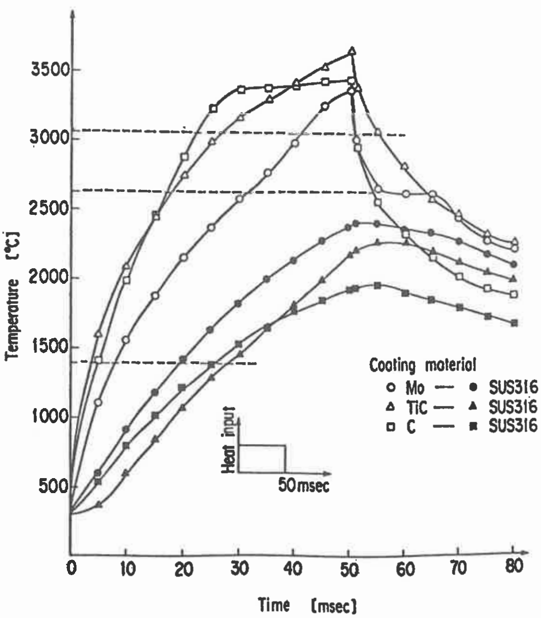

Fig. 5 Variation of melted zone
thickness with time

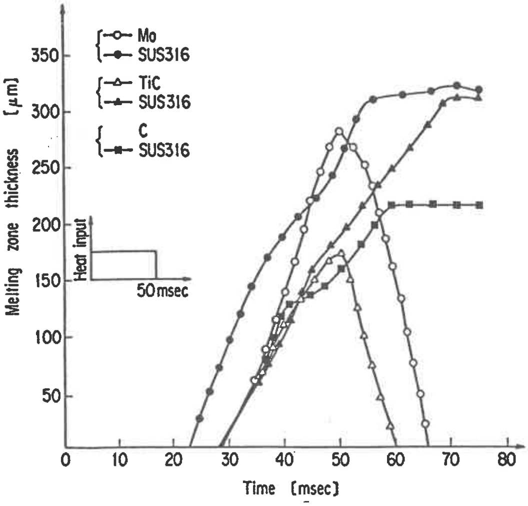

Fig. 6 Variation of evaporation thickness with time

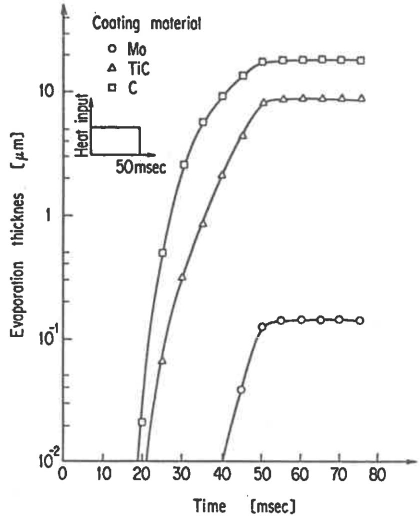

Fig. 7 Temperature change with time

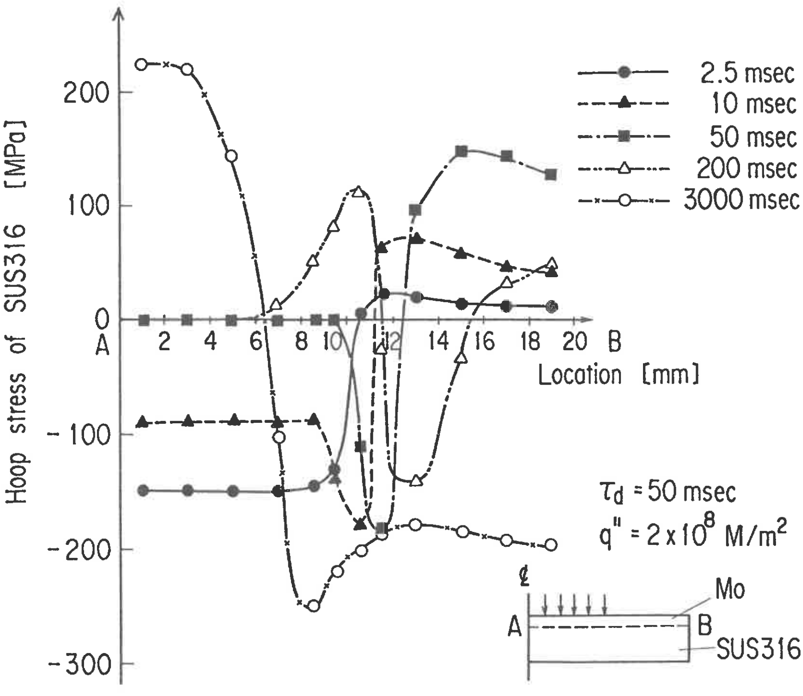

Fig. 8 Stress distribution of SS316 at various times